The effects of dosage and production process on the mechanical and physical properties of natural hydraulic lime mortars

Lucía Garijo[a], XiaoXin Zhang[1,a], Gonzalo Ruiz[a], José Joaquín Ortega[a], Zhimin Wu[b]

[a] ETS de Ingenieros de Caminos, Canales y Puertos, Universidad de Castilla-La Mancha, 13071 Ciudad Real, España.
[b] State Key Laboratory of Coastal and Offshore Engineering, Dalian University of Technology, 116024 Dalian, China.

ABSTRACT

Natural Hydraulic Lime (NHL) mortars are well-extended in restoration works presently. However, there is still a lack of standardization on their dosage methodology. Thus, seven types of mortar were fabricated and five factors which have an influence on their properties have been studied, in particular the water-binder ratio, the mold material, the aggregate size and type and the different curing conditions. Furthermore, an advanced mechanical characterization has been performed on these mortars, including the measurement of the fracture energy. Finally, some empirical equations for determining the relationships between these mechanical properties were proposed, which could be helpful when simulating the numerical models of historical constructions.

KEYWORDS: NHL mortar, Dosage, Mechanical Characterization, Fracture Energy, Empirical equations.

1. INTRODUCTION

Due to their good compatibility with the original material of ancient constructions and to their durability, lime-based mortars are used extensively in restoration works [1-4]. Despite their long track record, there is still a lack of standardization insofar as their dosage methodology and production process. Traditionally, the expression "1:3" has been used to define the dosage of a lime mortar. This expression is related with the binder-aggregate ratio by apparent volume and is also mentioned in the old treatises of Vitruvio, Alberti, Paladio and Benito Bails [5, 6]. This dosage method is the one traditionally used in construction due to its facility for measuring in blocks, buckets, or any other measuring instruments. It was not until the 19th century, that industrialization made the relationship between volume and weight proportions possible [6].

However, the matter of dosage has not been well-defined. For example, the amount of water was never indicated, despite its strong influence on mechanical properties. The physical properties, especially the density, of the materials in use (binder and aggregate) were not explained either. This fact absolutely complicates the matter of the dosage of lime

[1] Corresponding author: xiaoxin.zhang@uclm.es, zhangxiaoxinhrb@gmail.com.

mortars. The expression “1:3” can refer to slaked lime (aerial or hydraulic), lime putty, with river or crushed aggregate, and result in different weights [6].

Regarding the dosage or the factors affecting the fabrication process of lime mortars, Moropoulu *et al.* [7] recommended that the appropriate binder-aggregate ratio for restoration synthesis could be 1:3 by volume. Lanas and Alvarez [1] prepared aerial lime mortars with different binder-aggregate ratios, ranging from 1:1 to 1:5 by volume and studied their influence on the mechanical properties. In order to obtain normal consistency and good workability, the corresponding water-binder ratios were ranged from 0.5 to 1.2. They observed a correlation between binder amount and mortar strength. However, in the case of high binder contents, the increase in voids led to strength reduction. They also concluded that angular limestone improved the strength of the mortar. Gameiro *et al*. [8] studied the influence of binder-aggregate ratio on the physical and chemical properties of air lime-metakaolin mortars. The water-binder ratios were also varied to get adequate workability (consistency range: 129 mm -144 mm, from dry to plastic lime mortars). They found that mortars with low binder-aggregate ratio (1:3 by volume) seemed to develop carbonation sooner and therefore reach their highest strength relatively early while mortars with higher binder-aggregate ratio (1:1) presented lower carbonation rates. The latter is not appropriate for use in conservation works due to its high shrinkage and strong mechanical properties, which is incompatible with substrate material.

Referring to NHL mortars, Kalagri *et al*. [9] investigated the effect of aggregate size and the binder type on microstructure and mechanical properties, the water-binder ratio by weight was between 0.49 and 0.61, the consistency was 160 mm for all the mixes. The experimental results showed that coarse aggregates enhanced the compressive and flexural strengths, increased the packing density, decreased the water demand and consequently, reduced the open porosity. They also proposed an equation in regard to the compressive strength and the median pore radius. Moreover, Lanas *et al*. [10] studied the influence of binder-aggregate ratios and aggregate attributes on the mechanical properties of NHL mortars. They prepared five different binder-aggregate ratios from 1:1 to 1:5 in terms of volume and four different types of aggregates. The consistencies were from 128 mm to 159 mm by varying the water-binder ratio. They observed that specimens with more binder content had higher compressive and flexural strengths and, additionally, the highest strengths were reached with limestone aggregates.

As for the influence of water content, a general tendency was observed by Papayianni and Stefanidou [11], Xu et al. [12]. As the water-binder ratio increases, the porosity increases and as a consequence, the mechanical properties decrease, that is to say, the mortar becomes weaker.

Furthermore, there are other aspects, such as the material of the molds used and the different curing conditions, which also affect the fabrication process of NHL mortars. No research has been performed on the former. However, for the latter, Lanas *et al*. [13] fabricated the aerial and hydraulic lime-based mortars and subjected them to different environments. They concluded that, in general, higher relative humidity (RH) increased the mechanical properties of NHL mortars. Grilo *et al*. [14] studied the mechanical and mineralogical properties of natural hydraulic-metakaolin mortars under different curing conditions. They observed that lower humid conditions favored a carbonation reaction (which governed aerial lime mortars), while high humid curing aided a hydration reaction (which partially governed NHL mortars). Thus, they concluded that humid conditions (95 ± 5%) favored compound hydration and pozzolanic reactions, which were relevant for the development of mechanical properties of NHL mortars. Grilo *et al*. [15] also agreed that higher RH curing regimes benefited these processes and also contributed to void infilling.

However, the study of the influence of all these factors on the fracture properties of NHL mortars, like fracture energy and characteristic length, is not so well-documented. In our previous work [16], the effect of two water-binder ratios (0.8 and 1.1) on mechanical properties of NHL mortars were studied alongside with the influence of shape and size. The results show that there was an apparent size effect on the compressive strength, that is, the value measured from prism was much larger than that from cylinder, the ratio could reach 1.6. In addition, there are no empirical equations for the mechanical properties of these mortars as the ones proposed by the FIB Model Code [17] and ACI Building Code [18] for concrete. Thus, the aim of the paper is to determine the influence of different factors (water-binder ratio, type and size of aggregate, curing condition and material of mold) affecting the dosage and fabrication process of NHL mortars on the mechanical properties, including the compressive strength of prisms and cylinders, the flexural strength, the splitting tensile strength, the elastic modulus and the fracture energy. Furthermore, some empirical formulas determining a relationship between these properties and the compressive strength are proposed for the first time.

The rest of the paper is organized as follows. The next section describes the experimental procedure. In Section 3 a thorough analysis of the results and discussion are provided in addition to formulas which establish relationships between the mechanical properties of NHL mortars. Finally, our conclusions are presented in Section 4.

2. EXPERIMENTAL PROCEDURE

2.1. Raw materials

The binder used for all seven types of NHL mortar was a commercial lime of class NHL 3.5, in accordance with EN 459-1 [19] and was supplied by "Socli, Italcementi Group" (France). It had a density of 2580 kg/m^3 and an apparent density of 850 kg/m^3. Different aggregates were used as well. The common one was a commercial crushed limestone with a maximum grain size of 4 mm. In addition, crushed limestone with a maximum grain size of 2 mm and river sand with a maximum grain size of 4 mm were also used in the fabrication of various mortars. The particle-size distribution curve of aggregates, determined according to EN 1015-1 [20], is presented in Fig.1.

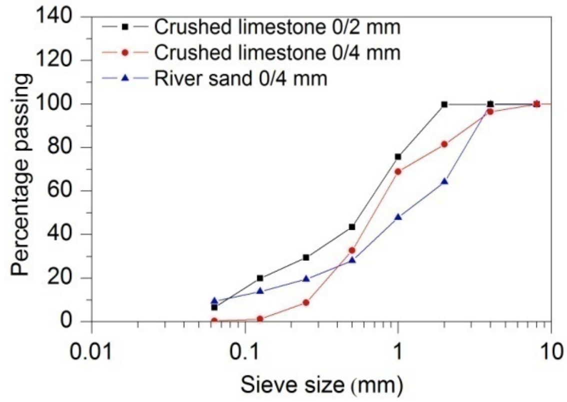

Figure 1. Aggregates grading curves.

The apparent particle density and the apparent density of each type of aggregate are listed in Table 1, in accordance with the standards EN 1097-6 [21] and EN 1097-3 [22], respectively.

Table 1. Apparent particle density and apparent density of each type of aggregate.

	Apparent particle density (kg/m^3)	Apparent density (kg/m^3)
Standards	EN 1097-6 [21]	EN 1097-3 [22]
Crushed limestone 0/4 mm	2680	1820
Crushed limestone 0/2 mm	2740	1810
River sand 0/4 mm	2590	1460

2.2. NHL mortar preparation

In total, seven types of NHL mortar were prepared and tested (see Table 2). First, as a reference material, a NHL mortar with a binder-aggregate ratio of 1:3 by volume was fabricated according to the traditional treatises and the recommendations of the references mentioned in Section 1 [5, 7, 11, 14]. A water-binder ratio of 0.9 by volume for the mortar was selected to obtain a plastic consistency from 140 mm to 200 mm, determined by the flow table test, in accordance with the standards EN 1015-3 [23] and EN 1015-6 [24]. It should be noted that the volume proportions of the compounds were converted to weight in order to obtain a convenient measurement for the mixing process. In addition, a crushed limestone aggregate with a maximum grain size of 4 mm and a metallic mold were used. For purpose of simplification, this benchmark NHL mortar was labeled NHL09C04M. The other mortar compositions were obtained by modifying an aspect of this material. For instance, NHL08C04M and NHL11C04M were achieved by changing the water-binder ratio of the benchmark to 0.8 and 1.1, respectively. Thus, dry, plastic and fluid mortars were obtained.

In order to disclose the influence of the type and size of sand, materials of mold and curing conditions on the mechanical properties of mortars, the water-binder ratio was kept constant as 0.9 to isolate and quantify the function of each factor. It is worth noting that we did not follow the conventional ideas for studying the effect of the type and size of sand, that is, maintaining the consistencies of mortars approximately constant by varing the water-binder ratios [1, 8-10, 13]. NHL09C04W was fabricated in wooden (plywood) molds (see Fig. 2) instead of the metallic one required by the standard EN 1015-11 [25]. NHL09C02M had the same type of crushed limestone aggregate, but with a maximum grain size of 2 mm. NHL09R04M was prepared with river sand. NHL09C04MA had the same composition as NHL09C04M, but was cured under the ambient laboratory conditions (RH of 50% ± 10% and 23ºC ± 3ºC) until the day of testing, after an initial seven days curing period in a climatic chamber at RH of 97% ± 0.5% and 20ºC ± 0.5ºC in accordance with the standard EN 1015-11 [25]. The remainder were cured in the climatic chamber until the day of testing.

The mixing process was performed according to the standard EN 1015-2 [26]. For each NHL mortar, 18 prisms (40 mm × 40 mm × 160 mm) and 6 cylinders (75 mm in diameter and 150 mm in height) were fabricated, followed by 126 prismatic specimens and 42 cylinders in total. All the molds were previously lubricated with mineral oil to prevent the mortar from adhering to the mold walls. The mortar was poured in two layers when using the prismatic molds and in three layers instead when using the cylindrical ones and each was compacted with 25 strokes of the tamper. All the specimens were removed from the molds in two days after the fabrication following the standard EN 1015-11 [25].

Table 2. Characteristics of the seven mortar compositions.

Mortar composition	Water-binder ratio (by volume)	Type of aggregate	Maximum grain size (mm)	Material of the mold	Curing conditions
NHL09C04M	0.9	Crushed limestone	4	Metallic	Climatic chamber
NHL08C04M	0.8	Crushed limestone	4	Metallic	Climatic chamber
NHL11C04M	1.1	Crushed limestone	4	Metallic	Climatic chamber
NHL09C04W	0.9	Crushed limestone	4	Wooden	Climatic chamber
NHL09C02M	0.9	Crushed limestone	2	Metallic	Climatic chamber
NHL09R04M	0.9	River sand	4	Metallic	Climatic chamber
NHL09C04MA	0.9	Crushed limestone	4	Metallic	Ambient laboratory conditions

Note: Climatic chamber (RH: 97% ± 0.5%, 20ºC ± 0.5ºC), Ambient laboratory conditions (RH: 50% ± 10%, 23ºC ± 3ºC)

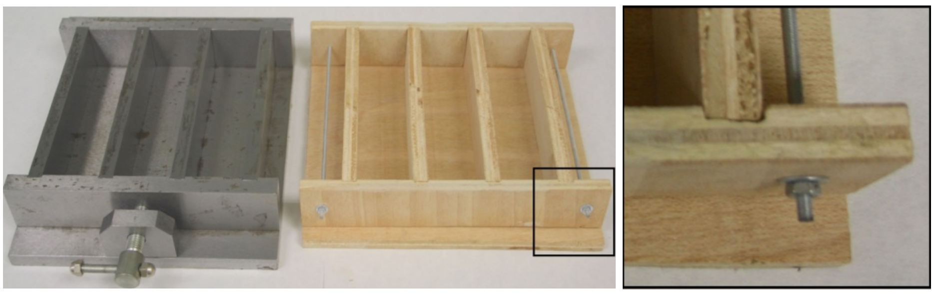

(a) Metallic mold (b) Wooden mold

Figure 2. Different types of molds for the fabrication of mortar.

2.3. Test of the NHL mortar in a fresh state

In a fresh state, the apparent density was measured following the standard EN 1015-6 [24]. The water-retention capacity was obtained according to the standard EN 459-2 [27], which was expressed as the percentage of water that remained in the mortar after a short suction time on a filter paper. In addition, the consistency was measured using the method mentioned in Section 2.2.

2.4. Mechanical tests on the NHL mortars

All the specimens were weighed and measured prior to testing. The flexural, compressive and splitting tensile strengths, the elastic modulus and fracture energy were obtained through various types of tests as shown in Fig. 3, at an age of 56 days.

2.4.1 Flexural and compressive strengths

The flexural and compressive strengths were determined according to the standard EN 1015-11 [25] by using an Instron 1011 testing machine. The flexural strength was measured by a three point-bending test on three beams (40 mm × 40 mm × 160 mm) at a loading rate of 10 N/s and a span of 100 mm, see Fig. 3(a). It is worth noting that the beam rests on two rigid-steel cylinders placed on two supports which permit rotation out of the plane of the beam and rolling along the longitudinal axis of the beam with negligible friction. That is, the anti-torsion supports were used for the test, which is specially important for quasi-brittle materials, like NHL mortars.

The compressive tests were conducted on the six half-prisms remaining from the bending tests at a loading rate of 50 N/s, as shown in Fig. 3(b). The load was centered in the middle of the longest side by using a steel plate (40 mm × 40 mm × 10 mm). Moreover, an individualized ball-and-socket joint over the steel plate was used to reduce the eccentricity during the loading process.

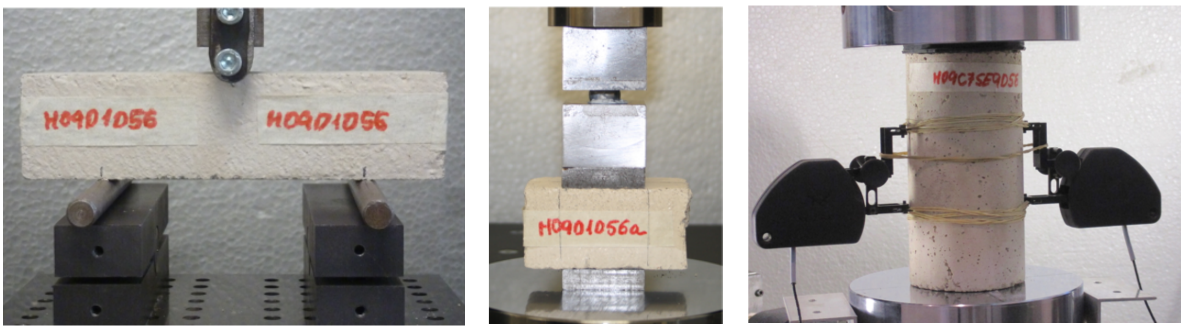

(a) (b) (c)

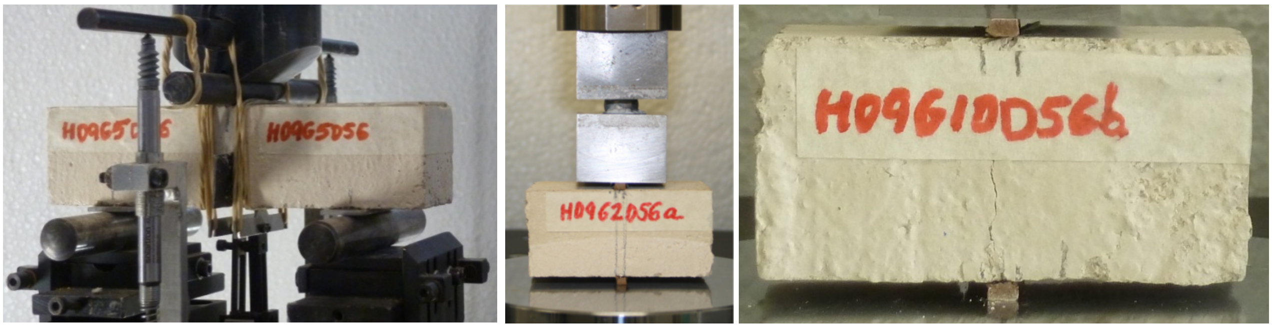

(d) (e) (f)

Figure 3. Test for: (a) flexural strength (b) compressive strength (c) elastic modulus and compressive strength (d) fracture energy (e) splitting tensile strength. (f) Crack pattern after splitting tensile test.

2.4.2 Compressive strength on cylinders and elastic modulus

In order to study the size and shape effects on compressive strength, compressive tests were also carried out on four cylinders (75 mm in diameter and 150 mm in height) at a loading rate of 10 N/s by using an Instron 8805 testing machine. In addition, the elastic modulus was measured in accordance with the principles of the standard EN 12390-13 [28], see Fig. 3(c). Two clips (strain gauge extensometers Instron 2630) centered on opposite generatrices were used to measure the axial deformation. The clips were placed covering a span of 50 mm so that local constrictions caused by the friction between the steel platens and the cylinder surface did not influence the measurement of the elastic modulus. Two rubber layers with 2 mm thickness each were used between the upper surface of the sample and the steel platen to avoid contact problems due to the irregular roughness of the sample. After measuring the elastic modulus, the specimens were broken to obtain the compressive strength.

2.4.3 Fracture energy

The fracture energy, G_F, was measured by a three-point bending test following the procedure recommended by RILEM [29] and the improvements proposed by Planas, Guinea and Elices [30-32]. For sake of convenience, the prisms were the same size as those used for the flexural tests. A pre-cast notch in the middle of the specimens was introduced by using a cardboard piece (2 mm in width and 20 mm in depth) during the fabrication. Four tests were conducted for each mortar.

The tests were performed by using an Instron 8805 testing machine as shown in Figure 3(d). G_F was obtained as:

$$G_F = \frac{W_m + W_{um}}{B(D-a)} \quad (1)$$

where W_m, measured energy, is the area under the experimental load–displacement curve (P_m–δ_m), and W_{um} is the unmeasured energy that corresponds to the portion of the ligament that is still unbroken when the test is stopped. B and D are the specimen width and depth, respectively. a is the notch depth.

We assume that the crack propagation obeys a cohesive model, which leads to a hyperbolic tail in the *P*–*δ* curve when displacement is very large and the ligament is very short [31, 33, 34]. Figure 4 shows the process used to obtain complete fracture energy, where δ_u and P_u correspond to the termination point of the bending test. It should be emphasized that the kinetic energy of the specimen is very small and insignificant compared with the fracture energy in our tests [34]. The procedure described above allows getting a size independent value for G_F [33].

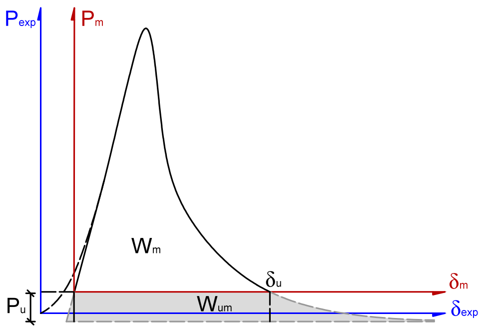

Figure 4. Determination of the fracture energy.

The weight-compensation technique was followed during the test in order to obtain complete failure information from the specimen, i.e. rubber bands were used to hold the specimen at all times, as shown in Figure 3(d). The specimen was placed over two rigid steel cylinders that could roll along the longitudinal axis of the specimen over supports that permit rotation out of the plane of the specimen. These supports were affixed to a steel beam attached to the machine frame. The loading point displacement in relation to this steel beam was measured by using two LVDTs (linear variable differential transducers) affixed to it. The tests were performed in position-control at a loading rate of 5.0×10^{-4}mm/s until a displacement equal to 0.3 mm and at 2.5×10^{-3} mm/s during the rest of the test (until reaching a displacement of 3 mm in total).

In addition, an extensometer (strain gauge extensometer Instron 2620) attached to the lower surface of the beam was used to obtain the crack-mouth opening displacement (CMOD). For span/depth (*S/D*) ratios (β) between 2.5 and 16, the elastic modulus obtained from prisms (E_{pr}) could be calculated by general Eqs. (2) and (3) according to the reference [35].

$$E_{pr} = 6\frac{Sa}{C_i B D^2}\upsilon_\beta(\alpha) \quad (2)$$

$$\upsilon_\beta(\alpha) = \upsilon_\beta(a/D) = 0.8 - 1.7\alpha + 2.4\alpha^2 + \frac{0.66}{(1-\alpha)^2} + \frac{4}{\beta}(-0.04 - 0.58\alpha + 1.47\alpha^2 - 2.04\alpha^3) \quad (3)$$

where C_i is the initial compliance determined from Load-CMOD curve, $\upsilon_\beta(\alpha)$ is a dimensionless shape function depending on β and the relative notch/depth ratio α. The other parameters of the beam have been previously defined.

It is worth noting that Eq. (3) changes to Eq. (4), which is recommended by RILEM TC 89-FMT for calculating the shape parameter [36] when the span/depth ratio β equals 4.

$$\upsilon_4(\alpha) = \upsilon_4(a/D) = 0.76 - 2.28\alpha + 3.87\alpha^2 - 2.04\alpha^3 + \frac{0.66}{(1-\alpha)^2} \quad (4)$$

2.4.4 Splitting tensile strength

Splitting tensile strength (indirect tensile strength) was measured through quasi-static splitting tensile tests (Brazilian tests) on four prismatic halves resulting from the preceding bending test for measuring fracture energy, in accordance with the procedures recommended by the standard EN 12390-6 [37]. To perform the test, the Instron 1011 testing machine was used, and the loading rate was set at 50 N/s. The proportion between the load-bearing width and the height of the specimens was maintained as low as 1/10 following the recommendations in [38-40]. The bearing strips were made of plywood, and they were placed in the middle of the longest side of the halves. The splitting tensile strength is obtained as:

$$f_t = 2F/\pi BD \quad (5)$$

where f_t is the splitting tensile strength, F is the maximum load, B and D are the specimen width and depth, respectively, as mentioned previously.

2.4.5 Characteristic length

Once splitting tensile strength (f_t), elastic modulus from cylinders (E_{cy}) and fracture energy (G_F) are obtained, the characteristic length, l_{ch}, can be calculated according to Eq. (6). It is a parameter proposed by Hillerborg *et al.* [41] for fracture behavior. It is related to the length of the Fracture Process Zone and could be used to predict the brittleness of a material. As it decreases, brittle nature dominates and vice versa [40].

$$l_{ch} = E_{cy} G_F / f_t^2 \quad (6)$$

2.5. Porosity and capillary water absorption measurements

Porosity is a key parameter for the evaluation of compatibility between original materials and restoration materials due to the fact that it mainly affects water movement and evaporation [42]. In the study, the open porosity at an age of 56 days was measured by a hydrostatic method following the standard UNE 83980 [43].

Furthermore, by means of the Mercury Intrusion Porosimetry (MIP) method, the pore-size distribution was obtained by using a Micromeritics 9500 Poresizer mercury porosimeter. This technique is based on the principle that a sample surrounded by mercury, a non-wetting liquid, fills its pores with mercury by applying pressure. The volume of the intruded mercury is subsequently recorded. At the lowest filling pressure, intrusion is considered zero and no pore volume of interest is filled. The volume of mercury required to fill all accessible pores is considered the total pore volume [44]. The percentage of porosity is obtained as Eq. (7).

$$\mathrm{P} = 100(V_{Pt}/V) \quad (7)$$

where V is the bulk volume of a sample (obtained from the bulk density) and V_{Pt} is the total intrusion volume [44]. Moreover, the pore size ranging from 0.003 to 300 μm can be detected by the MIP method.

The capillary water-absorption coefficient was measured according to the standard EN 1015-18 [45]. This test consists of drying halves of the prismatic samples, then, painting the four lateral surfaces with paraffin wax, and finally, immersing the cut surface in water for a period of time. Thus, the water-absorption coefficient *C* can be calculated according to Eq. (8):

$$C = 0.1\ (M2\text{-}M1) \quad (8)$$

where *M1* and *M2* are the mass in grams of the sample after 10 and 90 minutes of immersion, respectively. The unit of C is $kg/(m^2 min^{0.5})$.

3. RESULTS AND DISCUSSION

In this section the results of the experimental campaign described in Section 2 are presented. Table 3 provides a comparison between some of the experimental results obtained from other researchers and the results of this paper. Table 4 exhibits the properties of NHL mortars in a fresh state, while Table 5 presents the mechanical and physical properties of the seven NHL mortars in a hardened state. Std. Dev. is the standard deviation, and CV is the coefficient of variation.

From Table 3, it is important to note that the experimental results are similar among mortars which resemble one another in composition. For instance, the mortars tested by Drougkas *et al*. [46] and the mortar NHL09C04MA in the current work, were both mainly cured under ambient laboratory conditions. For the former, the flexural strength and the compressive strength are 0.8 MPa and 1.9 MPa, respectively, while they are 0.91 MPa and 2.4 MPa for the latter. Only a small difference is observed, which could be due to the different curing conditions during the first 7 days of maturation. In our case, it was cured in a climate chamber instead of under laboratory conditions. Moreover, similar mechanical properties were obtained by Grilo *et al.* in [14] compared with NHL09R04M in the current work, both of which had the same type of siliceous river sand. Furthermore, Maravelaki-Kalaitzaki *et al*. [47] prepared and tested a NHL mortar with pozzolanic additions by reproducing the original mortars from a historic masonry in Crete, Greece. The overall similarities obtained on the mechanical and physical properties of NHL09C04M may show that the fabricated mortar is also suitable for repairing historic masonry.

Table 3. Comparison of experimental results.

	Drougkas *et al*., 2015 [46]	Current work NHL09C04MA (ambient curing)	Grilo *el at.,* 2014, [14]	Current work NHL09R04M (river sand)	Maravelaki-Kalaitzaki *et al*., 2005, [47]	Current work NHL09C04M (benchmark)
NHL type	NHL 3.5	NHL 3.5	NHL 3.5	NHL 3.5	NHL-Z 3.5*	NHL 3.5
Aggregate type	Crushed limestone	Crushed limestone	Siliceous river sand	Siliceous river sand	Siliceous sand	Crushed limestone
Maximum grain size (mm)	5	4	-	4	5	4
Binder-aggregate ratio	1:3 by volume	1:3 by volume	1:3 by volume	1:3 by volume	6:14 by weight	1:3 by volume
Consistence (mm)		150-155	151-153	180-187	155	150-155
Curing conditions	(70.2% , 22.5ºC)	7 days at (RH 97±0.5%, 20±0.5ºC) and (RH 50±10%, 23±3ºC) until testing	(RH 95±5%, 20±3ºC)	(RH 97±0.5%, 20±0.5ºC)	3 days at (RH 95±1%, 20±1ºC) and (RH 60±1%, 20±1ºC) until testing	(RH 95±5%, 20±3ºC)
Age of testing	49 days	56 days	90 days	56 days	31 days	56 days
Flexural strength, f_{flex} (MPa)	0.8	0.91	1.2	0.96	-	1.3
Compressive strength, f_{cpr}(MPa)	1.9	2.4	2.4	2.3	3.48	3.2
Elastic modulus, E_{cv} (GPa)		1.5	-	4.2	7.12	5.0
Capillary water absorption coefficient (kg/(m^{2}min$^{0.5}$))	-	1.57	-	1.69	1.87	1.36
Open porosity (hydrostatic) (%)	-	29.0	-	29.4	26.23 (at 365 days)	27.7
Open porosity (MIP) (%)	-	23.8	-	24.0	-	23.4

*Natural hydraulic lime with pozzolanic additions.

Table 4. Properties of NHL mortars in a fresh state.

	NHL09C04M (benchmark)	NHL08C04M (water-binder: 0.8)	NHL11C04M (water-binder: 1.1)	NHL09C02M (maximum grain size: 2 mm)	NHL09R04M (river sand)
Flow diameter (consistence) (mm)	150-155	130-135	238-240	120-125	180-187
Category (consistence)	Plastic	Dry	Fluid	Dry	Plastic
Apparent density (g/cm^3)	2.25	2.29	2.24	2.25	2.11
Water retention (%)	83.5	90.9	76.7	91.6	78.7

Table 5. Properties of NHL mortars in a hardened state at an age of 56 days.

		NHL09C04M (benchmark)	NHL08C04M (water-binder: 0.8)	NHL11C04M (water-binder: 1.1)	NHL09C04W (wooden mold)	NHL09C02M (maximum grain size: 2 mm)	NHL09R04M (river sand)	NHL09C04MA (ambient curing)
Flexural strength, f_{flex} (MPa)	Mean	**1.3**	**1.3**	**0.89**	**1.7**	**1.1**	**0.96**	**0.91**
	Std. Dev.	0.1	0.1	0.04	0.1	0.1	0.06	0.02
	CV (%)	8	7	5	6	10	6	2
Compressive strength from prisms, f_{cpr} (MPa)	Mean	**3.2**	**4.2**	**1.7**	**3.5**	**3.2**	**2.3**	**2.4**
	Std. Dev.	0.1	0.3	0.1	0.1	0.2	0.1	0.1
	CV (%)	3	6	4	4	6	6	5
Compressive strength from cylinders, f_{ccy} (MPa)	Mean	**2.0**	**2.7**	**1.4**	-	**2.0**	**1.5**	**1.5**
	Std. Dev.	0.2	0.3	0.1		0.1	0.1	0.1
	CV (%)	9	12	8		7	8	3
Fracture energy, G_F (N/m)	Mean	**12**	**13**	**4.9**	-	**12**	**10**	**8**
	Std. Dev.	3	1	0.8		1	2	1
	CV (%)	22	9	17		10	19	10
Splitting tensile strength, f_t (MPa)	Mean	**0.39**	**0.51**	**0.24**	**0.57**	**0.49**	**0.38**	**0.34**
	Std. Dev.	0.02	0.01	0.03	0.05	0.05	0.03	0.03
	CV (%)	6	1	12	9	11	7	9
Elastic modulus from cylinders, E_{cy} (GPa)	Mean	**5.0**	**5.4**	**2.8**	-	**4.6**	**4.2**	**2.8**
	Std. Dev.	0.2	0.6	0.7		0.2	0.2	0.4
	CV (%)	4	10	25		4	6	7
Elastic modulus from prisms, E_{pr} (GPa)	Mean	**5.2**	**6.0**	**3.8**	-	**5.1**	**4.4**	**3.2**
	Std. Dev.	0.5	0.2	1.0		0.6	0.4	0.6
	CV (%)	11	3	27		11	8	18
Characteristic length, l_{ch} (mm)		**390**	**260**	**240**	-	**220**	**280**	**190**
Capillary water absorption coefficient (kg/(m^{2}min$^{0.5}$))	Mean	**1.36**	**0.95**	**1.70**	**1.83**	**1.84**	**1.69**	**1.57**
	Std. Dev.	0.06	0.07	0.07	0.03	0.03	0.07	0.06
	CV (%)	4	7	4	1	1	4	4
Open porosity (hydrostatic) (%)	-	**27.7**	**25.0**	**29.9**	**24.1**	**27.8**	**29.4**	**29.0**
Open porosity (MIP) (%)	-	**23.4**	**19.7**	**24.3**	**22.5**	**24.8**	**24.0**	**23.8**
Median pore radius (MIP) (µm)	-	**0.36**	**0.28**	**0.66**	**0.39**	**0.31**	**0.66**	**0.52**

From Table 5, it is obvious that there is considerable difference between the compressive strength from prisms and cylinders. For example, for NHL09C04M, they are 3.2 MPa and 2.0 MPa, respectively. The ratio between prism and cylinder strengths is 1.6, which is much larger than that of concrete [48]. The variations of density and open porosity of both specimens are less than 0.4%, which confirms that the fabrication process should not result in a such large difference. It is due to geometry and size effects [16, 48]. Similar tendency was also observed by Haach et al. [49] for cement-lime mortars, the ratio could reach 1.9. Moreover, for NHL09C04M, the elastic moduli are 5.0 GPa and 5.2 GPa measured from cylinders and prisms, respectively. The variation of both measurements is only 4%. However, for

NHL11C04M, the difference is greater (2.8 GPa versus 3.8 GPa), which may be mainly due to the quality or imperfections of the pre-notches. Nevertheless, they are still of the same order.

Regarding open porosity, due to the different ranges of pore-size detected, the values obtained by using the hydrostatic method are always greater than the ones measured by using the MIP method as presented in [50].

3.1 Influence of the water-binder ratio

Three types of mortars were tested in order to study the influence of the water-binder ratio on mechanical properties (NHL08C04M, NHL09C04M and NHL11C04M, with water binder-ratios of 0.8, 0.9 and 1.1, respectively). Their consistencies were dry, plastic and fluid, as shown in Table 4. In addition, the apparent density in a fresh state and the water-retention capacity increase as the water-binder ratio decreases. For example, for NHL08C04M, the apparent density and water-retention capacity are 2290 kg/m^3 and 90.9%, respectively, compared with 2240 kg/m^3 and 76.7% for NHL11C04M. In Table 5, it is observed that as the water-binder ratio increases, the open porosity increases as well, which causes a weakening of the material structure and its mechanical properties. This is attributed to the fact that both the carbonation rate of calcium hydroxide and calcium silicates hydrates in NHL paste present a downward tendency with an increase in the water-binder ratio [12].

Figures 5 and 6 show the pore-size distribution of seven types of NHL mortars measured by MIP in various ways. It is obvious that most of the mortars present a single narrow peak between 0.5 and 2 μm. A shift of the pore-size distribution towards a finer diameter is observed in mortar NHL08C04M, while in mortar NHL11C04M, there is a shift towards a larger one. Namely, with an increase in the water-binder ratio, the median pore radius also increases as shown in Table 5. This results in an increase of the capillary water-absorption capacity, which is the main controlling factor for determining service life. The higher the capillary absorption coefficients, the more vulnerable they are to the effect of ambient water and soluble salts [51, 52].

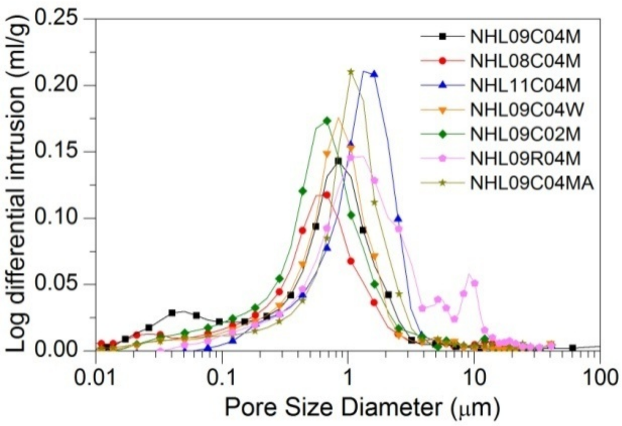

Figure 5. Pore-size distribution of NHL mortars as measured by MIP.

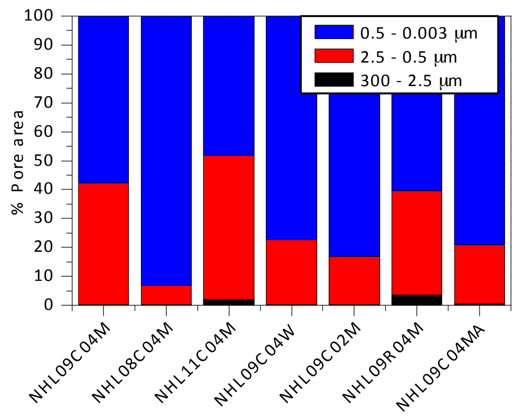

Figure 6. Pore-size distribution of NHL mortars as measured by MIP (percentage of pore area).

3.2. Influence of the material of the molds

In order to determine the influence of the material of the mold on the properties, a comparison was made between NHL09C04M and NHL09C04W mortars, fabricated with metallic and wooden molds respectively. The elastic modulus and the compressive strength of cylinders were not measured, as we did not make cylindrical wooden molds. In general, NHL09C04W exhibits a better mechanical behavior, see Table 5. For example, it has a flexural strength of 1.7 MPa and a compressive strength from prisms of 3.5 MPa. However for NHL09C04M they are instead 1.3 MPa and 3.2 MPa, respectively. This difference could be due to the fact that wooden molds absorb the excess of water from the mortar, and this absorption is local, which results in that the material is not going to be actually homogeneous. Accordingly, the water content of the specimens decreases compared with metallic molds. Thus, as mentioned in section 3.1, NHL09C04W has higher mechanical properties.

Moreover, due to the demolding process for the wooden molds (see Fig. 2), the nuts had to be removed from the steel wires, which caused damage in all the notched specimens. Thus, the fracture energy and the elastic modulus from prisms were not measured. Furthermore, all these molds were only used once for the fabrication of NHL mortars, as they supposedly change their absorption capability with each use, and therefore this would affect the comparison. Nevertheless, the influence of the material of the mold on the properties of mortars needs further study, research should examine the type of plywood used, the improvement of the demolding system and the possibility of reusing the molds.

3.3. Influence of the maximum aggregate size

Mortars NHL09C04M and NHL09C02M were prepared with the same composition but different maximum aggregate size (4 mm and 2 mm, respectively). The water-binder ratio was maintained at 0.9 for both. Thus, mortar

NHL09C02M had a lower consistency and a higher water demand in a fresh state, due to the fact that small aggregates could absorb more water during the fabrication process, i.e., it induces higher capillary water absorption coefficients in a hardened state [9, 53]. The influence of the aggregate size is coupled with the effect of the water-binder ratio. According to reference [9], larger coarse aggregates improve the resistance in a comparison among mortars with similar consistencies. However, this is achieved by means of adding water to mortars with smaller aggregates, as they have a higher water demand, which modifies the water-binder ratio. In our case, this proportion has been kept for NHL09C04M and NHL09C02M mortars, which results, respectively, in a plastic and a dry consistency in a fresh state (see Table 3). As both have similar mechanical properties, this could be explained by the positive effect of a lower water-binder ratio offsetting the possible lower capacity of smaller aggregates. Moreover, if more water were added to NHL09C02M to obtain a plastic mortar instead of a dry one, the mechanical properties should be weaker.

3.4. Influence of the aggregate type

The influence of two types of aggregate was studied by comparing NHL09C04M and NHL09R04M mortars, fabricated with crushed limestone and river sand, respectively. In a fresh state, NHL09R04M has a higher consistency (180-187 mm) than NHL09C04M (150-155 mm) for the same water-binder ratio. In addition, NHL09R04M has a lower apparent density and water-retention in a fresh state, see Table 4.

In a hardened state, NHL09R04M also presents lower mechanical properties than NHL09C04M (see Table 5). Moreover, the open porosity and the mean pore radius are higher for the former. Furthermore, NHL09R04M shows a high dispersion of the pore-size distribution with a broad curve (see Fig. 5) and presents the highest content of pores larger than 2.5 µm as well (see Fig. 6). These differences in the mechanical behavior and the size of the pores are mainly due to the interlocking of aggregate particles. Crushed limestone aggregates exhibit better interlocking behavior than river sands with round particles [1]. Undoubtedly, if less water were added to NHL09R04M to get similar consistency as NHL09C04M, the mortar would be stronger.

3.5. Influence of the curing conditions

The influence of the curing conditions has been studied between mortars NHL09C04M, cured in the climatic chamber (RH: 97%±0.5% and 20ºC±0.5ºC), and NHL09C04MA, cured under the ambient laboratory conditions (RH: 50%±10% and 23ºC±3ºC). It is observed in Table 5 and Fig. 5 that high RH favors lime hydration, which results in higher mechanical properties. NHL09C04MA shows 25% less compressive strength and 30% less flexural strength compared with those of NHL09C04M. Moreover, it has higher open porosity and median pore radius, 5% and 31%, respectively. Similar tendencies are also found in [13-15].

3.6. Characteristic length

As mentioned in Section 2.4.5, characteristic length is an indicator of brittleness of quasi-brittle materials. The shorter a material is, the more brittle it is. For all mortars studied in this paper, their range is from 190 mm to 390 mm, which is quite similar to the one of normal strength concrete (250 mm to 300 mm). Moreover, maximum grain size has a great impact on the parameter. For example, NHL09C04M and NHL09C02M, which have different maximum grain sizes (4 mm and 2 mm, respectively), present characteristic lengths of 390 mm and 220 mm, see Table 5. It is obvious that the smaller the aggregate size, the more brittle the mortar. Furthermore, using river sand in fabrication and curing under ambient laboratory conditions also make the mortar more brittle.

3.7. Empirical equations among mechanical properties

For the principal construction material, concrete, there are some recognized codes, such as the FIB Model Code [17] and ACI Building Code [18], which present empirical formulas relating compressive strength to other mechanical properties. These equations are quite helpful for numerical simulation and structural design when only compressive strength is measured due to the convenience of conducting the test, although relative error may be as high as 90% [54]. To our knowledge, there are still no empirical equations on mechanical properties of lime mortar, thus, according to the experimental results of seven types of mortar several Eqs. (9-14) are proposed as follows. It should be emphasized that the compressive strength of prisms is used as the basis of all empirical equations as it is a normalized property in lime mortars and easier to be measured.

$$f_{ccy} = 0.76 f_{cpr}^{0.85} \quad (9)$$

$$f_{flex} = 0.60 f_{cpr}^{0.62} \quad (10)$$

$$f_t = 0.18 f_{cpr}^{0.78} \quad (11)$$

$$G_F = 4.19 f_{cpr}^{0.82} \quad (12)$$

$$E_{cy} = 1.89 f_{cpr}^{0.75} \quad (13)$$

$$E_{pr} = 2.66 f_{cpr}^{0.85} \quad (14)$$

The determination coefficient, R^2, is calculated according to Eq. (15), where y_i is the i^{th} value of the variable to be predicted, x_i is the i^{th} value of the explanatory variable, $f(x_i)$ is the predicted value of y_i and $\bar{y}$ is the mean.

$$R^2 = 1 - \frac{\sum_i (y_i - f(x_i))^2}{\sum_i (y_i - \bar{y})^2} \quad (15)$$

In most cases, R^2 is over 75% while, for the flexural strength, it is only 56%, due to the fact that the result of the specimens fabricated in the wooden mold does not follow the trend.

Figure 7 shows the relationship among the mechanical properties, such as the compressive strength from cylinders, flexural strength, tensile strength, fracture energy and elastic modulus with respect to the compressive strength from prisms. It is worth noting that only the flexural strength and the splitting tensile strength are included for the mortar NHL09C04W, i.e., the specimen fabricated with wooden molds, as the rest were not measured.

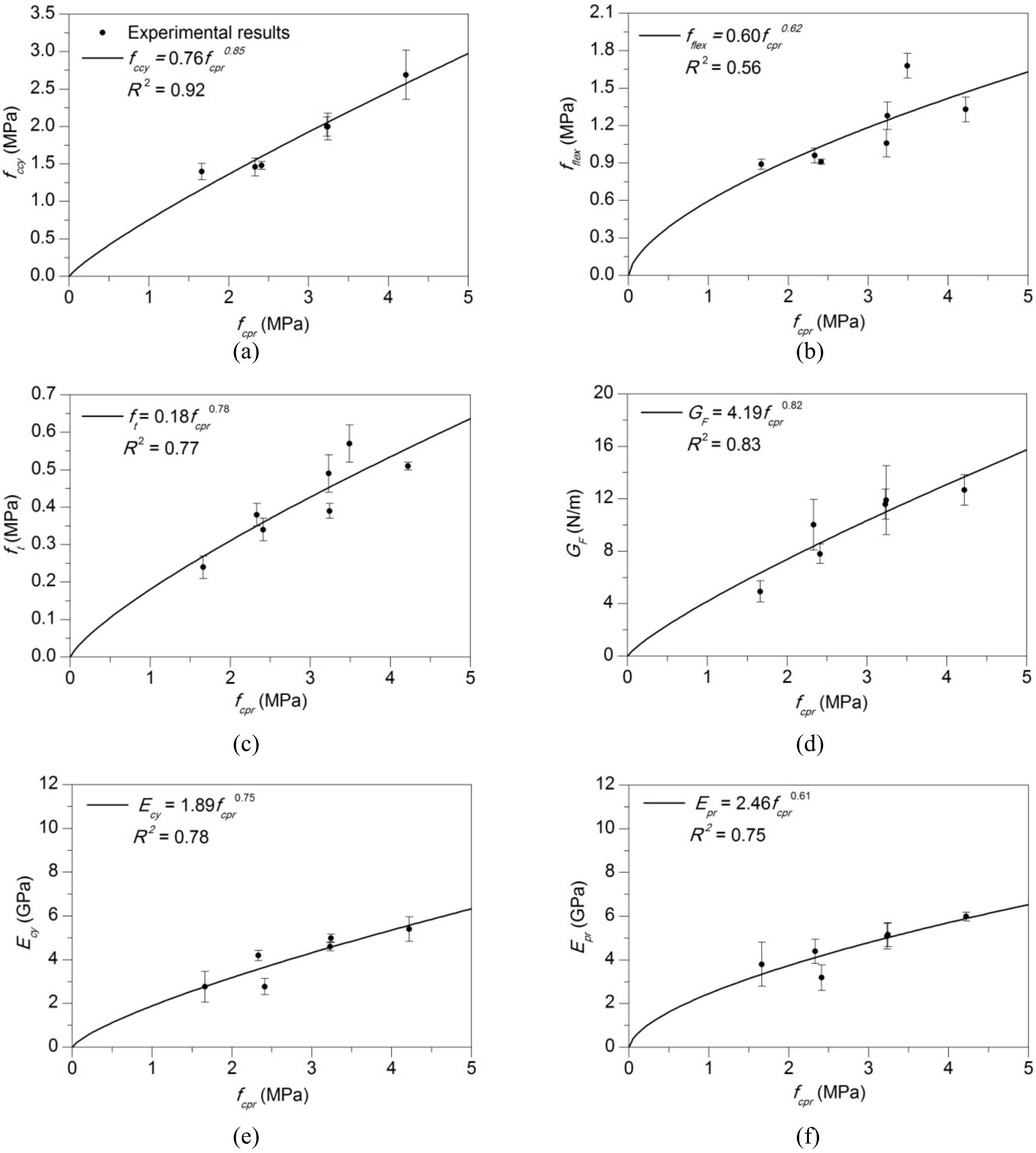

Figure 7. Relationship between the compressive strength from prisms and other mechanical properties: (a) compressive strength from cylinders, (b) flexural strength, (c) splitting tensile strength, (d) fracture energy, (e) elastic modulus from cylinders and (f) elastic modulus from prisms.

4. CONCLUSIONS

This work studied the influence of five factors affecting the dosage and fabrication process of NHL mortars on their mechanical and physical properties, such as water-binder ratio, wooden or metallic molds, aggregate type and size and curing condition. In total, seven types of NHL mortars have been fabricated and tested to obtain their mechanical properties, i.e., compressive strength from prisms and cylinders, flexural strength, elastic modulus from cylinders and prisms, fracture energy and splitting tensile strength. Moreover, some physical properties were also measured, such as open porosity, pore size distribution and capillary water absorption.

The experimental results show that high water-binder ratios produce structural weakening, increase the open porosity and reduce mechanical properties. High relative humidity (97% ± 0.5%) is more suitable than ambient laboratory conditions for the hydration of the compounds of NHL mortars and for the increase of its ductility. Moreover, it has been shown that the mortars fabricated with wooden molds obtain higher mechanical properties due to the fact that the molds absorb the excess of free water. However, this results in a non-homogeneous material, since the beneficial effect can be restricted to the material close to the mold surface.

When the water-binder ratio is fixed instead of maintaining the consistencies approximately constant by varying the water-binder ratios, the influence of type and size of aggregate on mechanical properties would be isolated and quantified. The mortar with an aggregate size of 2 mm has a lower consistency in a fresh state and smaller pore-sizes in a hardened state compared with the one with an aggregate size of 4 mm, due to the fact that small aggregates are more water demanding. Mortars with river sand have lower mechanical properties, higher pore radius and open porosity in comparison with the ones with crushed limestone aggregates. Undoubtedly, if the water-binder ratios varied as well, the tendency could be different.

Furthermore, some empirical equations which describe the relationship between the mechanical properties of the mortars and the compressive strength of the prisms are proposed. They are helpful for the characterization of lime mortars, as one of the main components of masonry, when simulating the mechanical behavior of historical constructions and monuments.

ACKNOWLEDGEMENTS

The authors wish to thank the funding from INCRECYT and the *Ministerio de Economía y Competitividad,* Spain, BIA2015-68678-C2-1-R. Lucía Garijo also acknowledges financial support from the scholarship FPU014/05186 awarded by the *Ministerio de Educación, Cultura y Deporte,* Spain and José Joaquín Ortega from the scholarship 2017/759 awarded by the *Junta de Comunidades de Castilla-La Mancha* (JCCM), Spain. We also express our gratitude to Prof. Pere Roca from *Universidad Politécnica de Cataluña* for his advice on the fabrication of NHL mortars, and Carlos Leiva from *Universidad de Sevilla* and Ángel de la Rosa from *Universidad de Castilla-La Mancha* for their help on the MIP technique.

REFERENCES

[1] Lanas J, Alvarez JI. Masonry repair lime-based mortars: Factors affecting the mechanical behavior. Cement and Concrete Research. 2003;33(11):1867-76.

[2] Elert K, Rodriguez-Navarro C, Pardo ES, Hansen E, Cazalla O. Lime mortars for the conservation of historic buildings. Studies in Conservation. 2002;47(1):62-75.

[3] Arizzi A, Viles H, Cultrone G. Experimental testing of the durability of lime-based mortars used for rendering historic buildings. Construction and Building Materials. 2012;28(1):807-18.

[4] Silva BA, Pinto APF, Gomes A. Natural hydraulic lime versus cement for blended lime mortars for restoration works. Construction and Building Materials. 2015;94:346-60.

[5] Bails B. Diccionario de Arquitectura Civil. Obra póstuma Madrid, Spain: Colegio de Aparejadores y Arquitectos Técnicos de Asturias, Oviedo; 1973.

[6] Rosell JR. Algunas consideraciones de la cal y sus morteros. II Jornadas FICAL. 2011:6-16.

[7] Moropoulou A, Cakmak AS, Biscontin G, Bakolas A, Zendri E. Advanced Byzantine cement based composites resisting earthquake stresses: the crushed brick/lime mortars of Justinian's Hagia Sophia. Construction and Building Materials. 2002;16(8):543-52.

[8] Gameiro A, Silva AS, Faria P, Grilo J, Branco T, Veiga R, et al. Physical and chemical assessment of lime-metakaolin mortars: Influence of binder:aggregate ratio. Cement & Concrete Composites. 2014;45:264-71.

[9] Kalagri A, Karatasios I, Kilikoglou V. The effect of aggregate size and type of binder on microstructure and mechanical properties of NHL mortars. Construction and Building Materials. 2014;53:467-74.

[10] Lanas J, Bernal JLP, Bello MA, Galindo JIA. Mechanical properties of natural hydraulic lime-based mortars. Cement and Concrete Research. 2004;34(12):2191-201.

[11] Papayianni I, Stefanidou M. Strength-porosity relationships in lime-pozzolan mortars. Construction and Building Materials. 2006;20(9):700-5.

[12] Xu SQ, Wang JL, Sun YZ. Effect of water binder ratio on the early hydration of natural hydraulic lime. Materials and Structures. 2015;48(10):3431-41.

[13] Lanas J, Sirera R, Alvarez JI. Study of the mechanical behavior of masonry repair lime-based mortars cured and exposed under different conditions. Cement and Concrete Research. 2006;36(5):961-70.

[14] Grilo J, Silva AS, Faria P, Gameiro A, Veiga R, Velosa A. Mechanical and mineralogical properties of natural hydraulic lime-metakaolin mortars in different curing conditions. Construction and Building Materials. 2014;51:287-94.

[15] Grilo J, Faria P, Veiga R, Silva AS, Silva V, Velosa A. New natural hydraulic lime mortars - Physical and microstructural properties in different curing conditions. Construction and Building Materials. 2014;54:378-84.

[16] Garijo L, Zhang XX, Ruiz G, Ortega JJ, Yu RC. Advanced mechanical characterization of NHL mortars and cohesive simulation of their failure behavior. Construction and Building Materials. 2017;153:569-77.

[17] FIB Model Code 2010, Final Draft. Lausanne, Switzerland: FIB-Fédération Internationale du Béton; 2012. p. 311.

[18] ACI 318-14. Building Code Requirements for Structural Concrete and Commentary. Farmington Hills: American Concrete Institute; 2014. p. 520.

[19] BS EN 459-1. Building lime – Part 1: Definitions, specifications and conformity criteria. Brussels, Belgium: BSI; 2015. p. 52.

[20] BS EN 1015-1. Methods of test for mortar for masonry – Part 1: Determination of particle size distribution (by sieve analysis): BSI; 1998/A1:2006. p. 8.

[21] BS EN 1097-6. Test for mechanical and physical properties of aggregates Part 6: Determination of particle density and water absorption: BSI; 2013. p. 54.

[22] BS EN 1097-3. Test for mechanical and physical properties of aggregates Part 3: Determination of loose bulk density and voids: BSI; 1998. p. 10.

[23] BS EN 1015-3. Methods of test for mortar for masonry – Part 3: Determination of consistence of fresh mortar (by flow table): BSI; 1999/A2:2006. p. 10.

[24] BS EN 1015-6. Methods of test for mortar for masonry – Part 6: Determination of bulk density of fresh mortar: BSI; 1998/A1:2006. p. 8.

[25] BS EN 1015-11. Methods of test for mortar for masonry – Part 11: Determination of flexural and compressive strength of hardened mortar: BSI; 1999/A1:2006. p. 12.

[26] BS EN 1015-2. Methods of test for mortar for masonry – Part 2: Bulk sampling of mortars and preparation of test mortars: BSI; 1998/A1:2006. p. 8.

[27] BS EN 459-2. Building lime – Part 2: Test methods: BSI; 2010. p. 68.

[28] BS EN 12390-13. Testing hardened concrete Part 13: Determination of secant modulus of elasticity in compression: BSI; 2012. p. 10.

[29] RILEM TC 50-FMC. Determination of the fracture energy of mortar and concrete by means of the three-point bend tests on notched beams. Materials and Structures. 1985;18:285-90.

[30] Elices M, Guinea GV, Planas J. Measurement of the fracture energy using three point bend tests. 3. Influence of cutting the P-δ tail. Materials and Structures. 1992;25:327-34.

[31] Elices M, Guinea GV, Planas J. Measurement of the fracture energy using three point bend tests. 1. Influence of experimental procedures. Materials and Structures. 1992;25:121-218.

[32] Planas J, Elices M, Guinea GV. Measurement of the fracture energy using three point bend tests. 2. Influence of bulk energy dissipation. Materials and Structures. 1992;25:305-12.

[33] Elices M, Guinea GV, Planas J. On the measurement of concrete fracture energy using three-point bend tests. Materials and Structures. 1997;30(200):375-6.

[34] Zhang XX, Ruiz G, Yu RC, Tarifa M. Fracture behaviour of high-strength concrete at a wide range of loading rates. International Journal of Impact Engineering. 2009;36(10-11):1204-9.

[35] Guinea GV, Pastor JY, Planas J, Elices M. Stress intensity factor, compliance and CMOD for a general three-point-bend beam. International Journal of Fracture. 1998;89(2):103-16.

[36] RILEM TC89-FMT. Determination of fracture parameters (KIcs and CTODc) of plain concrete using three-point bend tests. Materials and Structures. 1991;23:457-60.

[37] BS EN 12390-6. Testing hardened concrete – Part 6: Tensile splitting strength of test specimens: BSI; 2009. p. 14.

[38] Rocco C, Guinea GV, Planas J, Elices M. Size effect and boundary conditions in the brazilian test: Theoretical analysis. Materials and Structures. 1999;32(220):437-44.

[39] Iglesias I, Acosta B, Yu R, Ruiz G, Aineto M, Acosta A. Study of mechanical characterization of ceramic specimens from a brazilian test adaptation. Materiales De Construccion. 2011;61(303):417-29.

[40] Rocco C, Guinea GV, Planas J, Elices M. Size effect and boundary conditions in the Brazilian test: Experimental verification. Materials and Structures. 1999;32(217):210-7.

[41] Hillerborg A, Modéer M, Peterson PE. Analysis of crack formation and crack growth in concrete by means of fracture mechanics and finite elements. Cement and Concrete Research. 1976;6:73-782.

[42] Gulotta D, Goidanich S, Tedeschi C, Nijland TG, Toniolo L. Commercial NHL-containing mortars for the preservation of historical architecture. Part 1: Compositional and mechanical characterisation. Construction and Building Materials. 2013;38:31-42.

[43] UNE 83980. Concrete durability Test methods Determination of the water absorption, density and accessible porosity for water in concrete. Madrid: AENOR; 2014. p. 8.

[44] Stefanidou M. Methods for porosity measurement in lime-based mortars. Construction and Building Materials. 2010;24(12):2572-8.

[45] BS EN 1015-18. Methods of test for mortar for masonry – Part 18: Determination of water absorption coefficient due to capillary action of hardened mortar: BSI; 2002. p. 12.

[46] Drougkas A, Roca P, Molins C. Compressive strength and elasticity of pure lime mortar masonry. Materials and Structures. 2016;49(3):983-99.

[47] Maravelaki-Kalaitzaki P, Bakolas A, Karatasios I, Kilikoglou V. Hydraulic lime mortars for the restoration of historic masonry in Crete. Cement and Concrete Research. 2005;35(8):1577-86.

[48] del Viso JR, Carmona JR, Ruiz G. Shape and size effects on the compressive strength of high-strength concrete. Cement and Concrete Research. 2008;38(3):386-95.

[49] Haach VG, Vasconcelos G, Lourenço PB. Influence of aggregates grading and water/cement ratio in workability and hardened properties of mortars. Construction and Building Materials. 2011;25:2980-7.

[50] Silva BA, Pinto APF, Gomes A. Influence of natural hydraulic lime content on the properties of aerial lime-based mortars. Construction and Building Materials. 2014;72:208-18.

[51] Benazzouk A, Douzane O, Queneudec M. Transport of fluids in cement-rubber composites. Cement & Concrete Composites. 2004;26(1):21-9.

[52] Martys NS, Ferraris CF. Capillary transport in mortars and concrete. Cement and Concrete Research. 1997;27(5):747-60.

[53] Isebaert A, De Boever W, Descamps F, Dils J, Dumon M, De Schutter G, et al. Pore-related properties of natural hydraulic lime mortars: an experimental study. Materials and Structures. 2016;49(7):2767-80.

[54] Zhang XX, Ruiz G, Yu RC, Poveda E, Porras R. Rate effect on the mechanical properties of eight types of high-strength concrete and comparison with FIB MC2010. Construction and Building Materials. 2012;30:301-8.